# Photochemistry of "Super" Photoacids. 3. Excited-State Proton Transfer from Perfluoroalkylsulfonyl-Substituted 2-Naphthols[1]

**Caroline Clower,[†] Kyril M. Solntsev,*[,†,‡] Janusz Kowalik,[†] Laren M. Tolbert,*[,†] and Dan Huppert[‡]**

*School of Chemistry and Biochemistry, Georgia Institute of Technology, Atlanta, Georgia 30332-0400, and School of Chemistry, Raymond and Beverly Sackler Faculty of Exact Sciences, Tel Aviv University, Tel Aviv 69978, Israel*

*Received: July 18, 2001; In Final Form: December 18, 2001*

As a continuation of our efforts in the synthesis and investigation of novel "super" photoacids, in this article we report on the effect of fluoroalkanesulfonyl groups on the photoacidity of 2-naphthol. These groups, known to be the strongest electron-withdrawing substituents, were expected to increase the photoacidity to a greater extent as compared to previously described cyano- and methanesulfonyl groups. Indeed, we have found that 6-perfluoromethylsulfonyl-2-naphthol (**6F3**) is more acidic in the ground state and noticeably more acidic in the excited state than is previously synthesized 6-cyano-2-naphthol. The unusually short fluorescence lifetimes of the naphthol and the conjugated anion, which are explained by effective resonance/intramolecular charge transfer, mask the extended photoacidity of **6F3**. Photochemical investigations of 6-perfluorohexylsulfonyl-2-naphthol (**6F13**) in protic solvents are complicated by aggregation.

## Introduction

Photoacid generators, compounds that produce acids upon irradiation, are important because of their wide range of applications. In photosensitive polymeric systems, photoacid generators are used as initiators,[2] cross-linkers,[3] or in the conversion of acid-sensitive functional groups.[4] Particularly valuable technical applications include the production of photoresists and UV curing materials.[5] A significant drawback to conventional ionic photoacid generators is the mechanism of their action that is based on an irreversible chemical reaction. An alternate approach involves the design of transient photoacid generators, which produce acids only for the duration of the photochemical event then after relaxation to the ground-state return to their neutral form, allowing better control of the resulting chemistry. Thus in our search for more acidic photoacids, we now report the use of perfluoroalkylsulfonyl substitution and describe consequences of the resulting behavior of the naphthols.

Our interest in photoacids stems from the observation that hydroxyarenes (ROH) such as 2-naphthol (**N2**) and its derivatives undergo an enhancement in acidity upon photoexcitation, as measured by $pK_a^* > pK_a$ and predicted by the Förster equation:

$$pK_a^* = pK_a + \frac{\Delta E_{0,0}}{2.3RT} \quad (1)$$

This equation relates changes in acidity to a spectral shift between the acid and the base, measured by $\Delta E_{0,0}$. In the presence of a suitable proton acceptor B (see Figure 1[6]), a rapid excited-state proton transfer (ESPT) occurs, manifested by the appearance of two fluorescence bands from the emissions from the neutral (R*OH) and anionic ($R^*O^-$) forms of the excited naphthol. The corresponding shift of the anionic emission to longer wavelengths, relative to that of the neutral form ($h\nu_1 > h\nu_2$), makes 2-naphthol derivatives ideal substrates for examining fundamental aspects of intermolecular proton transfer using steady-state and time-resolved techniques.

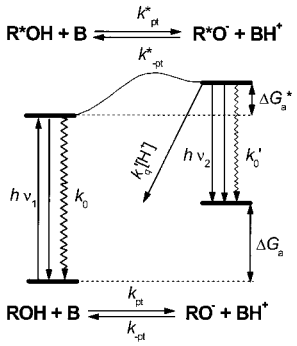


**Figure 1.** Energy scheme of excited-state proton transfer in naphthols.

Naphthols substituted in the distal ring with electron-withdrawing groups exhibit significant enhancement in acidity upon excitation,[7] for which Weller coined the term "intramolecular electron transfer".[8] For such molecules, excited-state proton transfer is observed even in nonaqueous solvents. Over the past decade, we have systematically expanded this class of "super" photoacids by synthesizing a series of naphthol derivatives strategically substituted with cyano and methanesulfonyl substituents.[9] The enhanced acidities of these substituted naphthols appear to follow a Hammett relationship, that is, systems substituted with functionalities of large positive Hammett constants ($\sigma_p$) behave as stronger photoacids (proton donors). Both the cyano- and methanesulfonyl substituents, with Hammett constants of 0.70 and 0.73,[10] respectively, increased the photoacidity of their parent naphthols. It follows that we can expect substitution with other electron-withdrawing sub-

* To whom correspondence should be addressed. E-mail: solntsev@chemistry.gatech.edu. Tel: (404) 894-4078. Fax: (404) 894-7452.
† Georgia Institute of Technology.
‡ Tel Aviv University.

10.1021/jp012774n CCC: $22.00 
Published on Web 03/13/2002

stituents, such as perfluoromethylsulfonyl ($\sigma_p = 1.08$),[11] to exhibit even further enhancement in photoacidity.

Previously, we have described the synthesis and fluorescent study of 6-perfluorohexylsulfonyl-2-naphthol (**6F13**).[12] Initial observations of steady-state fluorescence emission of this compound in methanol suggest that in alcohols aggregation occurs, which leads to significant fluorescence quenching. X-ray crystallography confirms that several cooperative attractive interactions are present in the crystal lattice, which are sufficient to effectively deactivate fluorescence in the solid state. No fluorescence quenching or aggregation is observed in nonpolar, weakly polar, and nonprotic solvents, such as hexane, ethyl acetate, and acetonitrile, respectively.[13]

In this article, we describe the synthesis of the short-chain analogue, 6-perfluoromethylsulfonyl-2-naphthol (**6F3**), with the aim of increasing its solubility in protic and aprotic polar solvents. We also present the results of our investigation of the mechanism of proton transfer from both **6F13** and **6F3** in MeOH/$H_2O$ mixtures by means of steady-state and time-resolved fluorescence emission. To reveal the effect of perfluoroalkylsulfonyl substitution of 2-naphthol, we compare spectral and kinetic properties and ESPT reactivity of **6F13** and **6F3** with that of other 6-substituted 2-naphthols, namely, 6-cyano-2-naphthol (**6CN2**) and 6-sulfonate-2-naphthol (**6SN2**).

## Experimental Section

**Materials.** Methanol (MeOH) and water were spectroscopic grade, purchased from Aldrich, and did not contain fluorescent impurities. All synthetic starting materials and reagents were commercially available and used without further purification. Synthesis of perfluoroalkylsulfonyl naphthols is described in Appendix 1.

**Absorption Measurements.** Absorption spectra were acquired with a Perkin-Elmer Lambda 19 UV/Vis/NIR spectrometer in dilute solutions in 1-cm cells. Solutions were prepared immediately prior to spectral measurements. Concentrations were in the range of $10^{-4}-10^{-5}$ M, typically 40 $\mu$M. The same solutions were used later for fluorescence measurements.

**Steady-State Fluorescence Measurements.** At the Georgia Institute of Technology, fluorescence spectra of nondeoxygenated solutions were recorded on a SPEX Fluorolog 112X spectrofluorometer equipped with a DataMax software system. At Tel Aviv University, fluorescence spectra were recorded on a SLM-AMINCO Bowman 2 luminescence spectrometer and were corrected according to manufacturer specifications.[7c] Sample fluorescence was collected at right angles from the excitation beam with monochromator entrance and exit slits of 1.0 mm. Spectra were acquired at room temperature.

Time-resolved fluorescence measurements were performed at Tel Aviv University and at the Laser Dynamics Laboratory of Professor M. E. El-Sayed at the Georgia Institute of Technology**.** To monitor ESPT in the time domain, the sample was excited by a picosecond laser at about 295 nm (the doubled frequency of the Rhodamine 6G dye laser, driven by an Nd/YAG laser). Using a time-correlated single-photon counting (TCSPC) system, transient fluorescence was collected at 370 nm (R*OH), followed immediately by a measurement at 515 nm ($R^*O^-$), which ensures that the time axes of the acidic and anionic fluorescence coincide. These wavelengths were chosen to minimize the overlap between fluorescence signals of protonated and dissociated forms of naphthols. The instrument response function (IRF) had a full width at half-maximum (fwhm) of about 40 ps. The full scale varied between 5 and 40 ns, corresponding to 4.88 and 39.1 ps/channel, respectively.

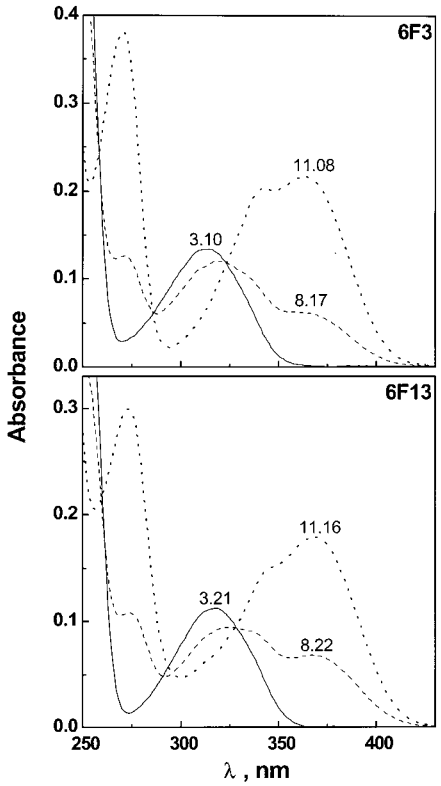


**Figure 2.** Absorption spectra of **6F3** (top) and **6F13** (bottom) in 50% v/v MeOH/$H_2O$ mixtures at various pH values (numbers on the graphs).

**TABLE 1: Properties of Perfluoroalkylsulfonyl-2-naphthols in 50% v/v MeOH/$H_2O$ Mixtures**

| | 2-naphthol | 6SN2 | 6CN2 | 6F3 | 6F13 |
|---|---|---|---|---|---|
| $\lambda_{max}$ (neutral, abs) | 329 | 280 | 302 | 314 | 319 |
| $\lambda_{max}$ (anion, abs) | 350 | 305 | 329 | 363 | 368 |
| $\lambda_{max}$ (neutral, em) | 360 | 365 | 375 | 400 | 395 |
| $\lambda_{max}$ (anion, em) | 425 | 430 | 435 | 442 | 425 |
| p$K_a$ | 10.5 | 9.7 | 8.8 | 8.47 | 8.4 |
| p$K_a$*[a] | 6.7 | 3.55 | 3.18 | −0.48 | −0.37 |
| p$K_a$*[b] | 3.1 | 2.6 | 0.95 | −0.06 | *c* |

[a] Calculated using eq 1. [b] Deterimined from the acid−base fluorescence titration. [c] Could not be determined (see text).

## Results

**p$K_a$ Measurements.** Because of the insolubility of **6F13** in water, all p$K_a$ experiments were conducted in 50% v/v MeOH/$H_2O$ solutions. Figure 2 shows the absorbance spectra of perfluoroalkyl naphthols at various pH values. The bands at 320 nm corresponded to ROH absorbance; with the pH increase, ground-state deprotonation resulted in a new bands around 370 nm. Ground-state p$K_a$ determinations were carried out by monitoring the pH dependence of $RO^-$ absorption. The sigmoid titration curves were fitted to a Boltzman function[14] using Microcal Origin version 5.0 software. Excited-state p$K_a$* values were estimated from absorption data using eq 1, where $\Delta E_{0,0}$ was approximated from the difference between the wavelengths of maximum absorption of the anionic and neutral forms. All experimental ground- and excited-state p$K_a$ values are listed in Table 1. We performed ground- and excited-state titrations of **6CN2** and **6SN2** as well as of the parent 2-naphthol in 50% v/v MeOH/$H_2O$ because these data are absent in the literature. The corresponding experimental acidity constants are collected in Table 1.

**Steady-State Fluorescence Spectroscopy.** All measurements were performed after slight acidification to pH $\approx$ 5 with HCl

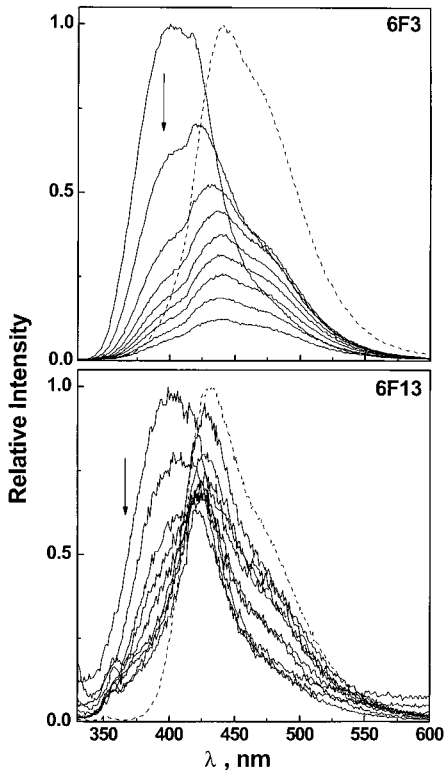


**Figure 3.** Effect of water on the emission of **6F3** (top) and **6F13** (bottom) in methanol. The arrow indicates increasing water concentration in increments of 0.1 from 0.0 to 0.8 volume fraction. The dashed curve is the emission resulting from direct excitation of the ground-state anionic form in methanol. Excitation wavelengths were 314 nm for **6F3** and 320 nm for **6F13**.

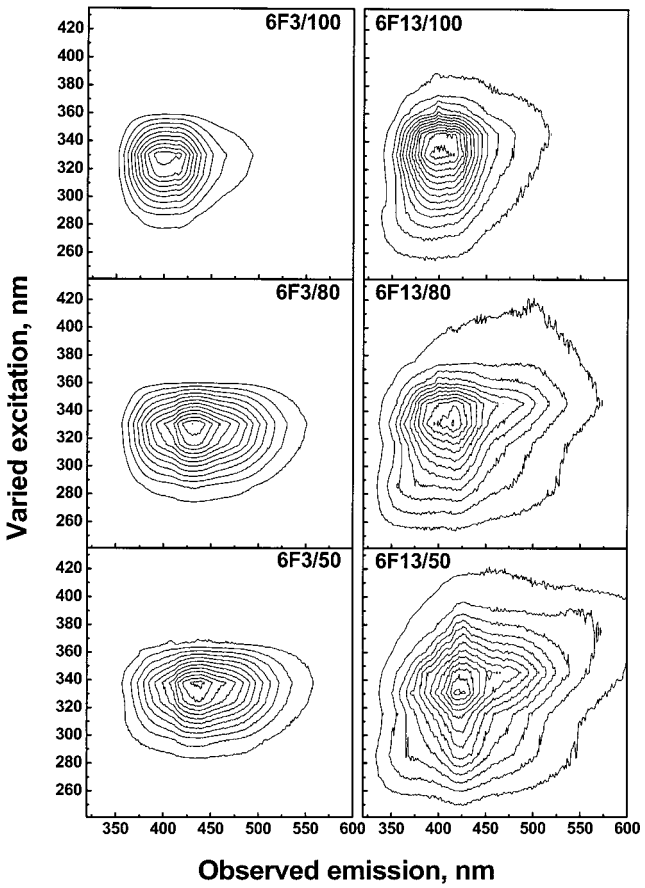


**Figure 4.** Contour plots of the emission of **6F3** and **6F13** at various excitation wavelengths in MeOH/$H_2O$ solutions. Abbreviations in each of the six graphs stand for naphthol name/volume percent of methanol in solution.

to ensure that only the ROH form existed in the ground state. The steady-state emission spectra of **6F3** in MeOH/$H_2O$ mixtures are shown in Figure 3. In pure methanol, a wide emission band with a maximum around 400 nm was observed, corresponding to the neutral form. The fluorescence quantum yield was about 0.05.[15] Upon the addition of water, the band decreased in intensity, and a new band with a maximum around 442 nm arose. This emission was attributed to the anionic form, as confirmed by the emission of pure naphtholate at high pH (Figure 3).[16] Such a small spectral separation between R*OH and R*$O^-$ is unusual for the naphthols. The emission spectra of **6F3** at various excitation wavelengths in MeOH/$H_2O$ solutions are shown on the left side of Figure 4. Regardless of the solvent, only one excitation peak was observed at 330 nm. The p$K_a$* of **6F3** was also determined using fluorescence titration by monitoring R*$O^-$ emission at 442 nm (data not shown). Attempts to determine the p$K_a$* of **6F13** by fluorescence titration were unsuccessful because of the low intensity and large overlap of emission spectra from the neutral and anionic forms (see below).

As with that of **6F3**, the steady-state emission spectrum of **6F13** in pure methanol consisted of a single band at about 395 nm, corresponding to emission from the neutral naphthol (bottom of Figure 3). However, the fluorescence quantum yield decreased by a factor of 10. In addition, the resonance light scattering from this solution was much larger, though no visible aggregation or opalescence was observed. This R*OH band of **6F13** decreased in intensity immediately upon the addition of water, and a new band began to develop with a maximum intensity at 425 nm that is consistent with emission from **6F13** in basic solution and is attributed to the naphtholate. Emission from the directly excited anionic form was as much as an order of magnitude more intense than that observed from neutral MeOH/$H_2O$ solutions at the same sample concentrations.

The emission spectra of **6F13** at various excitation wavelengths in MeOH/$H_2O$ solutions are shown on the right side of Figure 4. In pure methanol, emission from the neutral species at 395 nm was observed. As with the spectra of **6F3**, the addition of water resulted in a shift to anionic emission at 425 nm. However, additional peaks could be observed, producing an asymmetrical plot and complicated excitation curves. In 30% MeOH, slightly noticeable opalescence was observed in solution.

**Time-Resolved Fluorescence Spectroscopy.** Time-resolved emission spectra were measured at the corresponding wavelengths of the neutral (370 nm) and anionic (515 nm) species for both **6F13** and **6F3** in MeOH/$H_2O$ mixtures. A strong difference was observed in the water dependence of the time-resolved signals of **6F3** and **6F13**.

The fluorescence decay of **6F3** in pure MeOH at 370 nm was practically monoexponential, with a lifetime of 0.50 ns (Figure 5, top). The decay was independent of the detection wavelength. With the addition of water to this solution, the lifetime of R*OH measured at 370 nm rapidly decreased, and the decay became nonexponential. Moreover, the fluorescence decay measured at 515 nm demonstrated biexponential kinetics with rise and decay times that are typical for the excited-state reaction product, R*$O^-$ (Figure 5, bottom). With further increases of water concentration, both the R*OH and R*$O^-$ lifetimes decreased dramatically until the decay approached that of the lamp profile. In both R*OH and R*$O^-$ kinetics, a long-lived kinetic component with a lifetime of about 5 ns and a relative amplitude of less than 1% was observed at all water

**TABLE 2: Parameters Used in Fitting the Time-Resolved Fluorescence Decay of 6F3 and 6CN2 to Equations A1 and A2 and Calculated p$K_a$* Values in MeOH/$H_2O$ Mixtures[a]**

| vol % MeOH | mol % $H_2O$ | $k_d$, 1/ns | $k_a/4\pi a^2$, Å/ns | $k_q/4\pi a^2$, Å/ns | $\tau_0'$, ns[b] | $D$, $10^{-5}$ cm$^2$/s[c] | $R_D$, Å[c] | p$K_a$* [d] |
|---|---|---|---|---|---|---|---|---|
| 100 | 0 | <0.1[e] (<0.01)[e] | *f* | *f* | *f* | 3.66 | 17.20 | >3[g] (>4)[g] |
| 70 | 36 | 9 (1.9) | 18.5 (19) | 6 (3.1) | 0.28 (6.7) | 2.32 | 13.0 | 0.7 (1.39) |
| 50 | 69 | 17 (3.8) | 18.5 (25) | 25 (5) | 0.14 (6.3) | 4.07 | 9.57 | 0.15 (0.93) |
| 30 | 84 | 25 (5.7) | 18.5 (25) | 25 (8) | 0.10 (6.0) | 6.0 | 8.36 | −0.11 (0.66) |

[a] Data for **6CN2** is given in parentheses. At all concentrations, we have taken $a = 5.5$ Å and $\tau_0 = 0.5$ (4.5) ns. The relative error for the kinetic parameters is 10%. [b] Indirectly excited R*O$^-$. [c] From ref 1. [d] Calculated using eq A5. [e] Estimated to be $<0.05/\tau_0$. [f] No ESPT. [g] $k_a$ was assumed to be the same as that in MeOH/$H_2O$ mixtures.

**TABLE 3: Results of the Multiexponential Fit of 6F13 Time-Resolved Emission Data[a]**

| detection $\lambda$, nm | vol % MeOH | $\tau_1$, ns | $A_1/\Sigma A_i$ | $\tau_2$, ns | $A_2/\Sigma A_i$ | $\tau_3$, ns | $A_3/\Sigma A_i$ |
|---|---|---|---|---|---|---|---|
| 370 (R*OH) | 100 | 0.016 | 0.987 | 1.57 | 0.003 | 5.40 | 0.010 |
| | 100[b] | 0.020 | 0.996 | 1.14 | 0.002 | 5.80 | 0.002 |
| | 70 | 0.005 | 0.980 | 2.06 | 0.007 | 5.91 | 0.014 |
| | 50 | 0.008 | 0.877 | 1.96 | 0.076 | 5.43 | 0.047 |
| | 30[c] | 0.021 | 0.791 | 2.16 | 0.185 | 5.60 | 0.024 |
| detection $\lambda$, nm | vol % MeOH | $\tau_1$, ns | $A_1/(A_1 + A_2)$ | $\tau_2$, ns | $A_2/(A_1 + A_2)$ | $\tau_3$, ns | $A_3/(A_1 + A_2)$ |
| 515 (R*O$^-$) | 100 | | | | | | |
| | 70 | 0.010 | 0.967 | 10.6 | 0.033 | 1.07 | −0.014 |
| | 50 | 0.009 | 0.918 | 11.0 | 0.082 | 1.76 | −0.049 |
| | 30[c] | 0.093 | 0.831 | 10.1 | 0.169 | 4.44 | −0.051 |

[a] Kinetic curves $I(t)$ were measured with 39.1 ps/channel resolution (40 ns full scale). The relative error for the kinetic parameters is 10%. [b] Kinetic curves were measured with 4.88 ps/channel resolution. In this case, amplitudes for slower exponents were determined with better accuracy, and lifetimes, with worse accuracy. [c] Results are less reliable because of visible opalescence.

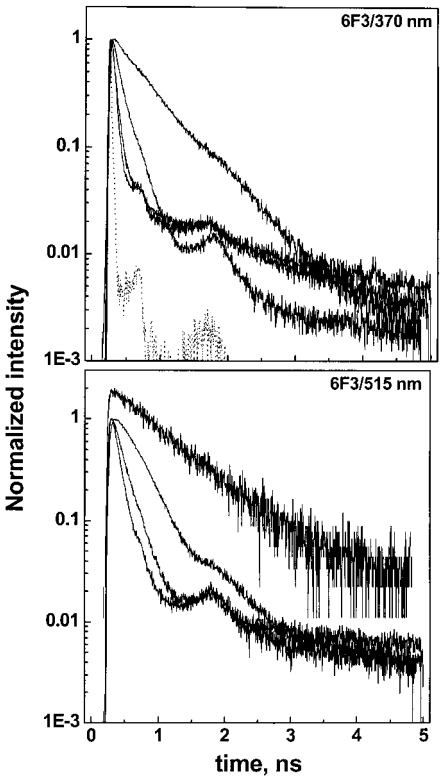


**Figure 5.** Time-resolved emission of **6F3** in MeOH/$H_2O$ solutions observed at 370 nm (top) and 515 nm (bottom). In each graph, a decrease of the effective lifetime from top to bottom corresponds to decreased methanol content: 100, 70, 50 and 30 vol % MeOH, respectively. The dashed line in the upper plot corresponds to IRF.

concentrations. As in previous work, we attribute this minor component to fluorescence from aggregates or impurities. Experimental curves were fitted to the numerical solution of the time-dependent Debye−Smoluchowski equation using the SSDP program/approach used previously.[17] This fitting procedure has been described in detail in our previous publications,[1,7c]

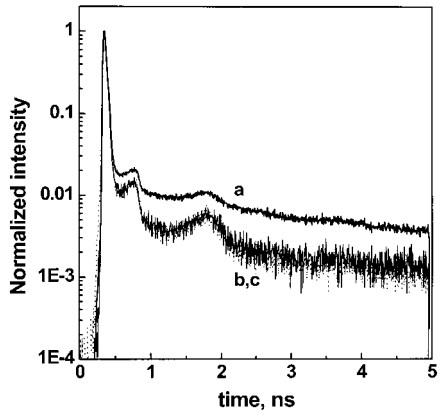


**Figure 6.** Time-resolved emission of **6F13** in pure methanol observed at (a) 370 nm, (b) 405 nm, and (c) 460 nm.

and in Appendix 2 we provide only the fundamentals of our method. The fitting parameters are presented in Table 2. Time-resolved measurements of **6CN2** in MeOH/$H_2O$ mixtures were also performed, and data was analyzed in the same manner. The results are given in Table 2, as well.

The time-resolved emission of **6F13** in pure methanol is shown in Figure 6. In contrast to **6F3**, two major components were detected regardless of the observation wavelength. The curves were fitted to a sum of three exponentials $I(t) = \sum_{i=1}^{3} A_i \exp(-t/\tau_i)$ after convolution with IRF.[18] From the amplitudes given in the fitting data (Table 3), we can estimate that at least 99% of the excited population decayed very rapidly. The determination of the lifetime of the dominating ultrafast compound was limited by the time resolution of our TCSPC system (about 20 ps). We made sure that this emission was not scattered light by varying the monochromator slits, wavelengths, and cutoff filters. As the water concentration increased, the R*OH decay profiles kept their bimodal nature without significant change of the lifetimes (Figure 7, top). The amount of the short-lived species decreased slightly but was still at least 97% of the original amount.[19] Monitoring the fluorescence decay at

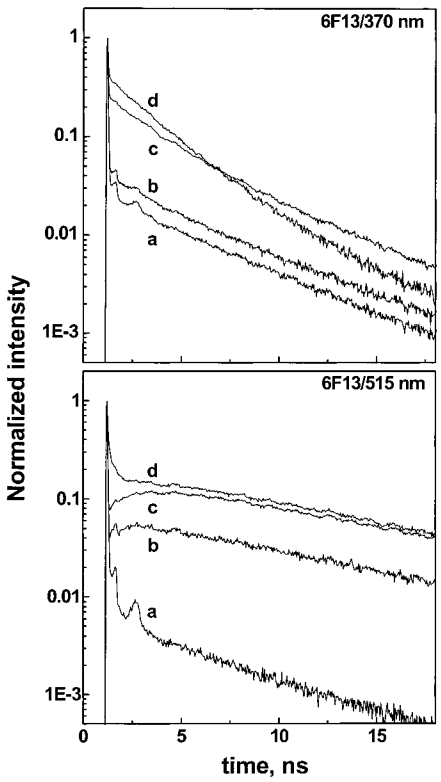


**Figure 7.** Time-resolved emission of **6F13** in MeOH/$H_2O$ solutions observed at 370 nm (top) and 515 nm (bottom). The volume percentage of methanol for each graph is (a) 100, (b) 70, (c) 50, and (d) 30.

the wavelength of the anion at 515 nm (Figure 7, bottom) in pure methanol did not show any rising components, as in the case of **6F3**, but instead still showed the predominance of the very fast component. Upon the addition of water, the ultrafast species was still a major component. However, a very unusual component with *slow* rise and decay times appeared. Its amplitude increased with water content (Table 3).

## Discussion

The ground-state p$K_a$ values showed only a small effect upon perfluoroalkylsulfonyl substitution or for variation in the length of the alkane chain, as expected for substitution distal to the hydroxyl group. The excited-state p$K_a$* values determined by the Förster equation must be considered to be approximate because solvent effects in the ground state differ greatly from those in the excited state. Even so, the estimated values suggest that the perfluoroalkylsulfonyl substituent does enhance the photoacidity of the naphthol. Indeed, the fluorescence emission titration of **6F3** results in a p$K_a$* of −0.06, proving that the photoacidity has increased over that of the cyano-substituted analogue (**6CN2**), which has a p$K_a$* of 0.95.

It was demonstrated by Bosch et al. that standard glass electrodes can be successfully used for pH measurements in MeOH/$H_2O$ solutions of different concentrations.[20] Very small differences (less than 0.15 pH units) were found for the pH values of a wide array of buffers in pure water and 50% v/v MeOH/$H_2O$.[20a] These same authors found that the p$K_a$ values of 28 substituted phenols at any MeOH/$H_2O$ composition are linearly related to the p$K_a$ values in water.[20c] The p$K_a$ values of 1- and 2-naphthols in 50% v/v MeOH/$H_2O$ solutions exceed the corresponding values in water by about 0.8 p$K_a$ units. Therefore, we can assume that the difference in the acidity constants for 6-substituted 2-naphthols observed in MeOH/$H_2O$ mixtures remains the same in pure water.

Neither 2-naphthol, **6SN2**, nor **6CN2** is capable of transferring a proton to pure methanol in the excited state. However, other monocyanoderivatives of **N2** such as 5- and 8-cyano-2-naphthol do dissociate in methanol while in their excited states with a rate of $k_d \approx 0.2$ ns$^{-1}$.[7c] We have found no evidence for the expected ESPT in methanol from **6F3** and **6F13** in steady-state or time-resolved signals. We consider several possible reasons for this result: From the kinetic measurement, we know that the fluorescence lifetime of **6F3** in pure methanol is 0.5 ns, which is shorter than R*OH lifetimes of various **N2** derivatives by a factor of 9−15, which includes the sum of the radiative and nonradiative rate processes. To be detected, the realistic difference between the fluorescence and another process should be several percent of $\tau_0$. In other words, all photochemical processes with rates less than $\sim 0.05/\tau_0$ go undetected. According to this estimation, the upper limit for the **6F3** dissociation rate constant is 0.1 ns$^{-1}$, which is a reasonable value because it increases this limit by a factor of 9 as compared to the upper limit for **6CN2** (Table 2). Changing the substituent from cyano to trifluoromethylsulfonyl probably increases the reactivity of naphthol, but very rapid deactivation masks this change.

The R*OH lifetime of **6F3** is not the only surprisingly short lifetime. With the addition of water, emission from the anion is observed both in the steady-state and time-resolved signals, indicative of proton transfer to solvent. It is interesting to note that the anionic lifetime is also unusually small and decreases with increasing water concentration (Table 2), which is consistent with the increasingly low R*O$^-$ intensity observed in Figure 3 and results in the absence of an isoemissive point. The lifetimes of this excited anion were much shorter than those of 2-naphthol and even 5-cyano-2-naphthol (**5CN2**), our fastest monosubstituted naphthol to date. We now consider possible ways of shortening the 2-naphtholate lifetime after *amphi* substitution (2:6). Quenching by geminate protons may lead to keto-structure A in Figure 8.[21] However, we have calculated[22] that the formation of this structure is energetically unfavorable (in contrast to C-5 protonation of the excited 1-naphtholate); moreover, the concentration of the geminate protons capable of recombining with the parent naphtholate anion is extremely low because of slow protolytic photodissociation. Nevertheless, structure A in Figure 8 suggests that substituents at the 6 position may delocalize the excited state in a manner similar to that of 5-substitution in 1-naphtholate. For the latter, *ana*-substituted (1:5) naphthols, we have recently observed a significant shortening of the R*O$^-$ lifetime.[23] Similarly, for 2-naphtholate, sulfonyl or cyano substituents may polarize the excited state, as indicated by species B, C, and D in Figure 8. Not all substituents may shorten the 2-naphtholate lifetime. For example, the lifetime of the 2-naphthol-6-sulfonate dianion in water is 15 ns,[24] which is longer than that of the parent 2-naphtholate, an effect that may be related to the anionic substituent. The small decrease in the lifetime of species D (Table 2) caused by cyano substitution demonstrates the increasing role of *intramolecular* electron transfer. The perfluoroalkylsulfonyl group introduced in this work is the strongest electron-withdrawing group reported for this system. We propose that the combination of these properties of the $CF_3SO_2$ group stabilizes resonance structure C, which leads to significant intramolecular fluorescence quenching in R*O$^-$ and, to some extent, in R*OH. Effective formation of the nonemissive intramolecular charge-transfer (ICT) state [25] is known for some aromatic molecules having electron donor and acceptor substituents. The efficiency of ICT formation (related to the nonradiative rate constant $k_{nr}$) increased with solvent polarity

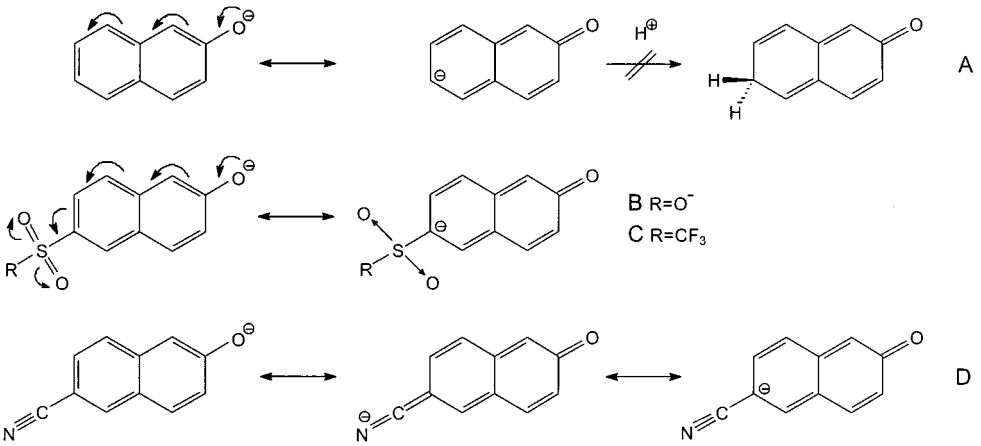


**Figure 8.** Possible molecular mechanisms (proton quenching and resonance stabilization) for the deactivation of 2-naphtholates.

($E_T$(30) parameter).[25] The same solvent dependence of $k_{nr}$ is observed for **6F3** in various solvents.[26] The nature of the excited state of perfluoroalkylsulfonyl naphthols is currently under investigation.

The shortening of the R*O$^-$ lifetime in 5-methanesulfonate-1-naphthol results in an unusual kinetic transition[23] that is predicted by theory.[27] Fast R*O$^-$ decay as compared to relatively slow ESPT in nonaqueous solvents leads to a switch from the power-law $t^{-3/2}$ R*OH asymptotic decay (AB regime) to the rising exponent (A regime).[28] Despite the ultrashort **6F3** R*O$^-$ lifetimes, the ESPT kinetic is still in the AB regime because of very fast photodissociation rates (Table 2). Comparison of the dissociation rate constants at various water concentrations with that of **6CN2** (Table 2) demonstrates that changing the substituent group from cyano to perfluoroalkylsulfonyl markedly increases the acidity of naphthol, making it comparable to the most acidic monosubstituted 2-naphthol, **5CN2**.[1] It is interesting to note that the ratio of $k_d$ and the difference in p$K_a$* for **6F3** and **6CN2** are independent of water concentration (Table 2).

**6F13** shows no ESPT in solvents of medium polarity and basicity, such as acetonitrile or ethyl acetate, having intensive R*OH fluorescence with quantum yields larger than 0.1. By contrast, steady-state emission spectra from the neutral species of **6F13** in protic or basic solvents (alcohols and THF) were notably weak, quenched by a factor of 40 compared to that of the nonfluorinated analogue, 6-hexanesulfonyl-2-naphthol,[12] and quenched by an order of magnitude compared to that of **6F3**. We suspect that aggregation of the molecules accounted for this low quantum yield. A Beer's law plot for **6F13** using the absorbance intensity of the neutral form at various concentrations was nonlinear above $10^{-4}$ M, confirming the presence of more than one species in the solution in the ground state (i.e., neutral and aggregate), which results in wide, asymmetrical, wavelength-dependent emission at all water concentrations, unlike the analogous plots for **6F3** (Figure 4). In addition, we have previously reported the existence of three intermolecular attractions of **6F13** in the solid state: hydrogen bonding between the hydroxy and sulfonyl groups, $\pi-\pi$ interactions, and F···F bonding between perfluorohexane chains.[12] Clearly, aggregation occurs in both the solid state and in solution, although the nature of the aggregates in solution is not obvious.

Because of the complex character of the molecule and the fact that the steady-state spectra of **6F13** were generally of low intensity and wavelength-dependent, time-resolved measurements were used to further investigate the nature of the neutral, anionic, and aggregate species. The emission at 370 nm (Figure 7) showed two major species present in the solution regardless of solvent composition. The first species underwent a very fast (ps) decay, with a lifetime close to the IRF response time, which accounted for 99% of the excited population in methanol; the remaining 1% had a 5.4 ns lifetime. As the volume fraction of water increased, the percentage of the fast decay decreased, showing that the nature of the aggregate changes with changes in the solvent. We were unable to analyze these kinetic data using the SSDP program because of dominating noninformative ultrafast decay. Some information, however, can be obtained from a multiexponential fit.

Observation at an anionic emission wavelength (515 nm, Figure 7) of the same solutions also showed the presence of multiple components. The vast majority of the excited population had a short (ps) lifetime, which again was reduced in percentage as the water concentration increased, and the remainder displayed more typical nanosecond decays. In pure methanol, the long lifetime was on the order of 6 ns. As the water concentration increased, a slow-rise component (>1 ns) with a long lifetime of 10.5 ns appeared.

To explain these phenomena, we consider the fact that the emission comes from two or more species varying in structure and probably in electronic properties as evidence of effective aggregation that has already been observed in the ground state (Figure 4, right side). It is tempting to assume that the shortest dominating exponent relates to **6F13** aggregates, in which effective quenching takes place, whereas long-lived exponents belong to monomer molecules. However, we have established that R*OH and R*O$^-$ fluorescence lifetimes of the short-chain analogue **6F3** are very short and tend to decrease with the increase of water concentration in the solution (Figure 5, Table 2). The perfluoroalkyl substituent is a stronger electron-withdrawing group in **6F13** than in **6F3**, so we assume that the effective fluorescence lifetimes of R*OH and R*O$^-$ in **6F13** should not be larger than those in **6F3**. Therefore, long-lived exponents could not belong to monomers; thus the dominating ultrafast component should belong to free molecules. The amplitude of these latter components decreases with increasing water concentration, which reasonably agrees with the increasing fraction of aggregates as the solvent becomes more polar.

Previously in the series of super photoacids articles, we faced the problem of naphthol aggregation regularly. We considered it an annoying and unavoidable side effect masking important long-time ESPT kinetics. In all cases, the fluorescence kinetics of such aggregates contained a decaying exponent with an average lifetime of 4−8 ns and a relative amplitude of less than 1% regardless of the observation wavelength. Surprisingly, for

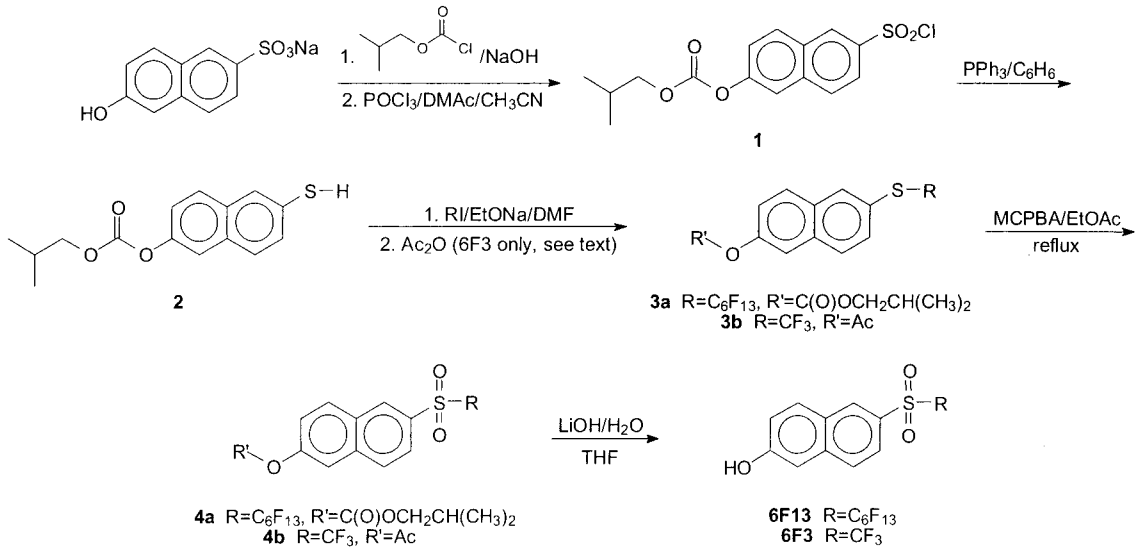


**Figure A1.** Synthesis of perfluoroalkylsulfonylnaphthols **6F13** and **6F3**.

**6F13** fluorescence kinetics in MeOH/$H_2O$ mixtures, we have observed a slow-rising component at the wavelength corresponding to anionic emission, with an amplitude much larger than those for other super photoacids (Table 3, Figure 7). This low-energy species formation is not attributed to proton transfer from the monomer because this process is expected to be very fast, comparable to the dissociation from **6F3**. Instead, this nanosecond process can be attributed to dissociation from the aggregate $*(ROH)_n$ to form an aggregation anion $*(ROH_{n-1})_n^-$. However, the more likely scenario is excimer decay because it is known that the lifetimes of the excimer fluorescence of the aromatic molecules are generally much longer than those of free molecules.

The possible formation of excimers is an unusual complication of ESPT studies. In a sense, an excimer is just an example of the excited aggregate $*(ROH)_n$ for which $n = 2$. In fact, other naphthyl-containing chromophores are known to exhibit excimer emission, with wavelength shifts comparable to those we would obtain for deprotonation.[29] In solutions of very hydrophobic **6F13**, the excited dimer can be obtained by direct excitation of the ground-state dimer (van der Waals complex) or by recombination of excited- and ground-state chromophores. We will not discuss the detailed mechanism of ground- and excited-state aggregation of **6F13** in the present article, but it is worth mentioning that both kinds of aggregation are possible in MeOH/$H_2O$ solutions of this molecule. Similar behavior was observed in water for 4-(1-pyrene)butanoate.[30] For this compound, the excimer-formation equilibrium constant increased significantly with the increase of water content in MeOH/$H_2O$ mixtures, which is in good agreement with the increasing fraction for slowly dissociating species in MeOH/$H_2O$ solutions of **6F13**. In this case, the integral contribution $A_3\tau_3/\sum_{i=1}^{3}A_i\tau_i$ of the slowest kinetic component into the fluorescence spectra reflects the emission from excimers (aggregates).

## Conclusions

Steady-state and time-resolved fluorescence spectroscopy involving excited-state proton transfer have been used to gauge the photoacidity of naphthol derivatives with perfluoroalkylsulfonyl substituents. These very strong electron-withdrawing substituents were shown to enhance the photoacidity of 2-naphthol much more than did other groups such as sulfonate or cyano. Unfortunately, utilization of the increased photoacidity of these novel super photoacids was complicated by efficient deactivation of **6F3,** which led to the shortening of its lifetime in both the protonated and deprotonated states and as a consequence decreased the photodissociation efficiency. In the case of **6F13**, the longer substituent chain causes aggregation in polar protic solvents, leading to quenching and complicated fluorescence spectra and kinetics. Nevertheless, such fluorinated super photoacids may be useful in studies involving fluorinated solvents and surfactants.

## Appendix 1

**Synthesis of 6F3 and 6F13. 6F13** and **6F3** were synthesized as depicted in Figure A1 and were briefly described previously.[12] 6-Hydroxynaphthalene-2-sulfonic acid was allowed to react with isobutyl chloroformate under Schotten−Bauman conditions to mask the hydroxy group.[31] The subsequent reaction with $POCl_3$[32] yielded the sulfonyl chloride (**1**), which was reduced with $PPh_3$ to obtain the thiol (**2**).[33] The thiol **2** was then allowed to react with perfluorohexyl iodide to yield the corresponding thioether **3a.** In the reaction of **2** with trifluoromethyl iodide, extensive O deprotection was observed, and the isolated product was 6-trifluoromethyl-2-thionaphthol, which was then re-acylated with acetic anhydride. The thioethers were then oxidized with 3-chloroperbenzoic acid to yield the corresponding O-acylated sulfones. Hydrolysis using lithium hydroxide in 50% $H_2O$/THF solution provided the desired naphthols **6F13** and **6F3**. The final products were recrystallized from hexanes, and their purity was checked by HPLC and GC. The purity of **6F13** was additionally confirmed by crystallography data.[12]

Newly synthesized perfluoroalkylsulfonylnaphthols were characterized by standard spectroscopic techniques. For the "nearly-first-order" $^1H$ NMR spectra, the proton−proton coupling constants in case of multiplets were taken directly from the spectra and were not optimized.

**Spectral Data. 6-Perfluorohexylsulfonyl-2-naphthol (6F13):** $^1H$ NMR (acetone-$d_6$, 300 MHz) $\delta$ 9.79 (s); 8.71 (s, 1H); 8.26 (d, 1H, $J_{HH} = 9.9$ Hz); 8.07 (d, 1H, $J_{HH} = 8.7$ Hz); 7.88 (dd, 1H, $J_{HH} = 8.7$ Hz, 2.4 Hz); 7.44 + 7.42 (s + dd, 2H, $J_{HH} = 7.5$ Hz, 2.7 Hz); IR (in KBr, $cm^{-1}$) 3467 (sharp, s); 1617 (s); 1466 (w); 1397 (s); 1385 (s); 1354 (s); 1246 (s); 1207 (vs); 1170 (s); 1146 (s); 1128 (m); 1113 (m); 1077 (w); 1047 (w);

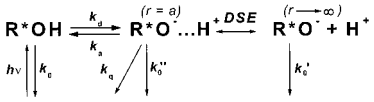


**Figure A2.** Two-step reaction scheme of ESPT from naphthols.

868 (w); 817 (w); 660 (w). EIMS *m*/*z* 526, 507, 443.1, 207, 159.1, 143.1 (100%), 89, 69; HRMS (FAB, *m*/*z*) calcd for $C_{16}H_8O_3SF_{13}$ $[M + H]^+$ 526.99866, found 526.99604; mp 133−135 °C (from hexanes).

**6-Trifluoromethylsulfonyl-2-naphthol (6F3):** $^1$H NMR ($CDCl_3$, 300 MHz) $\delta$ 8.55 (s, 1H); 7.97 (d, 1H, $J_{HH} = 8.7$ Hz); 7.88 (s, 2H, AB system); 7.31 (dd, 1H, $J_{HH} = 8.7$ Hz, 2.7 Hz); 7.27 (d, 1H, $J_{HH} = 2.4$ Hz); 6.12 (br s, 1H); IR (in KBr, $cm^{-1}$) 3690−2600 (br); 1618 (m); 1468 (w); 1397 (m); 1353 (m); 1211(vs); 1142 (s); 1129 (s); 1067 (m); 867 (w); 818 (w); 667 (m); 614 (m); EIMS *m*/*z* 276, 207, 191, 159.1, 143.1 (100%), 115.1, 102.1, 89, 69; HRMS (EI, *m*/*z*) calcd for $C_{11}H_7O_3SF_3$ 276.00680, found 276.00744; mp 114−116 °C (from hexanes).

## Appendix 2

**Diffusion Theory of ESPT in Naphthols.** Previously, we demonstrated experimentally and theoretically that a two-step reaction model (Figure A2) adequately describes the nonexponential fluorescence decay of some rapidly dissociating naphthols, particularly super photoacids.[1,7c,23,27] In this scheme, initially excited naphthol (R*OH) undergoes reversible photodissociation with a rate constant $k_d$, forming the solvent−contact-ion pair (CIP) $R^*O^-...H^+$. The solvent−ion pair can undergo both adiabatic and nonadiabatic recombination, with rate constants $k_a$ and $k_q$, respectively. The second step in Figure A2 involves diffusional separation of CIP from the contact radius, *a*, to infinity. It is described by the transient numerical solution of the Debye−Smoluchowski equation (DSE). Additionally, one should consider the fluorescence lifetimes of all of the excited species: $1/k_0 = \tau_0$ for the acid, $1/k_0' = \tau_0'$ for the base, and $1/k_0'' = \tau_0''$ for the CIP. Usually, $\tau_0''$ is much longer than that for all other chemical and diffusion processes and can be ignored.

According to Figure A2, the excited-state populations of naphthol and its anion can be represented by two coupled differential equations. The spherically symmetric Smoluchowski equation (eq A1) describes the probability density, $p(r, t)$, of CIP to separate to a distance *r* at time *t* after excitation in its bound excited state (R*OH), whereas the simple kinetic equation (A2) denotes the probability $P(t)$ of observing R*OH.

$$\frac{\partial}{\partial t}p(r,t) = \left[r^{-2}\frac{\partial}{\partial r}Dr^2e^{-V(r)}\frac{\partial}{\partial r}e^{V(r)} - k_0'\right]p(r,t) + [k_dP(t) - (k_a + k_q)\,p(r,t)]\frac{\delta(r-a)}{4\pi a^2} \quad \text{(A1)}$$

$$\frac{\partial}{\partial t}P(t) = k_a\,p(a,t) - (k_d + k_0)\,P(t) \quad \text{(A2)}$$

Here, $D = D_{H+} + D_{R^*O-}$ is the mutual diffusion coefficient of the proton and its conjugate base. The Coulomb attraction potential is $V(r) = -R_D/r$ where the Debye radius, $R_D$, at temperature *T* is given by

$$R_D \equiv |z_1z_2|e^2/(k_BT\epsilon) \quad \text{(A3)}$$

$z_1$ and $z_2$ are the charges of the proton and the base, respectively, and $\epsilon$ is the static dielectric constant.

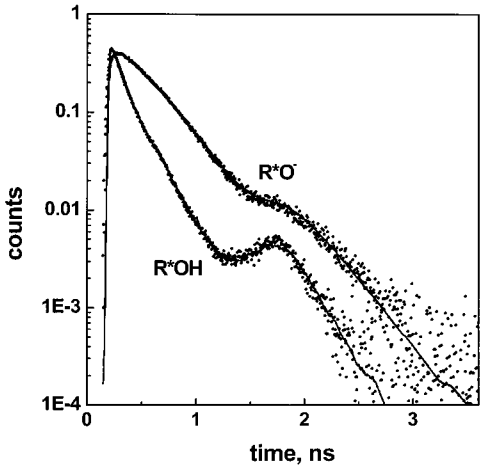


**Figure A3.** Time-resolved kinetics of **6F3** in 70:30 vol % MeOH/$H_2O$. Experimental data points (normalized to the theoretical amplitudes) are compared with the numerical solution of the DSE (lines), using the parameters of Table 2, after convolution with IRF.

In practice, we solve the system of the coupled partial differential equations (A1 and A2) numerically and compare the time-dependent R*OH signal with $P(t)$ and $R^*O^-$ with

$$S(t) = 4\pi\int_a^\infty p(r,t)\,r^2\,dr \quad \text{(A4)}$$

Usually, diffusion coefficients, Debye radii, and contact radii are estimated from literature values, whereas the excited-state lifetimes $\tau_0$ and $\tau_0'$ are determined from independent measurements at the conditions when ESPT is suppressed. As a result, only three kinetic parameters, $k_d$, $k_a$, and $k_q$, are varied. A detailed procedure of the fitting and parameters estimation is described in our previous publications.[1,7c,23] Finally, we note that the excited-state $pK_a^*$ can be calculated from the rate parameters according to

$$pK_a^* = -\log\frac{k_d10^{27}\exp(-R_D/a)}{k_aN_A} \quad \text{(A5)}$$

where the scaling factor $10^{27}/N_A$ converts Å$^3$/ns into mol/s.

Figure A3 shows an example of the experimental kinetic data fitting. Here, the dots are the time-resolved emission data for **6F3** in 70:30 vol % MeOH/$H_2O$, and the solid curves are the theoretical calculations for both the acidic and anionic forms of naphthol convoluted with IRF. All parameters used for the theoretical curves construction are given in Table 2. The experimental data are essentially the same as those given in Figure 5, except for long-time, long-lived exponential tails in both R*OH and $R^*O^-$ signals that were extracted in Figure A3. The lifetimes of these exponents were 4.5 ns for both R*OH and $RO^-$, and the relative amplitudes were 0.0022 for R*OH and 0.0049 for $R^*O^-$. As was discussed previously, these kinetic components do not relate to ESPT from **6F3** and appear as a result of aggregation and impurities. It is important to mention that both the R*OH and $R^*O^-$ kinetics were fitted simultaneously using the same kinetic parameters listed in Table 2.

**Acknowledgment.** We thank Victor Volkov (Georgia Institute of Technology) and Boiko Cohen (Tel Aviv University) for help with the time-resolved measurements and Noam Agmon for comments on the manuscript. Support of this research to L.M.T. by the National Science Foundation through grant number CHE-9727157 is gratefully acknowledged. D.H. ac-

knowledges support from the Israel Science Foundation and the James Franck Program for Laser−Matter Interaction.

## References and Notes

(1) For part 2, see Solntsev, K. M.; Huppert, D.; Agmon, N.; Tolbert, L. M. *J. Phys. Chem. A* **2000**, *104*, 4658.

(2) Wei, Y.; Wang, W.; Yeh, J. M.; Wang, B.; Yang, D. C.; Murray, J. K. *Adv. Mater. (Weinheim, Ger.)* **1994**, *6*, 372.

(3) (a) Harvard, J. M.; Yoshida, M.; Pasini, D.; Vladimirov, N.; Frechet, J. M. J.; Medeiros, D. R.; Patterson, K.; Yamada, S.; Willson, C. G.; Byers, J. D. *J. Polym. Sci., Part A: Polym. Chem.* **1999**, *37*, 1225. (b) Yu, H. S.; Yamashita, T.; Horie, K. *Macromolecules* **1996**, *29*, 1144. (c) Chae, K. H.; Park, I. J.; Choi, M. H. *Bull. Korean Chem. Soc.* **1993**, *14*, 614.

(4) (a) Kim, S. T.; Kim, J. B.; Chung, C. M.; Ahn, D. D. *J. Appl. Polym. Sci.* **1997**, *66*, 2507. (b) Chen, J. P.; Gao, J. P.; Wang, Z. Y. *J. Polym. Sci., Part A: Polym. Chem.* **1997**, *35*, 9. (c) Kim, H. K.; Ober, C. K. *Polym. Bull.* **1992**, *28*, 33.

(5) For a recent review, see Shirai, M.; Tsunooka, M. *Bull. Chem. Soc. Jpn.* **1998**, *71*, 2483.

(6) In this scheme, $k(*)_{pt}$ denotes proton-transfer rates in the ground (excited) state, $\Delta G_a(*) = 2.3RT\ pK_a(*)$ is the free energy of ground (excited) state proton transfer, $k_0$ and $k'_0$ are the fluorescence decay rates for acid and base, and $k'_q$ is the rate constant of proton quenching.

(7) (a) Weller, A. *Prog React. Kinet.* **1961**, *1*, 187. (b) Förster, T. *Pure Appl. Chem.* **1970**, *24*, 443. (c) Solntsev, K. M.; Huppert, D.; Agmon, N. *J. Phys. Chem. A* **1999**, *103*, 6984.

(8) Strictly speaking, this is an oxymoron for electron redistribution. However, given its wide usage in the literature, we will continue this term.

(9) (a) Tolbert, L. M.; Haubrich, J. E. *J. Am. Chem. Soc.* **1994**, *116*, 10593. (b) Huppert, D.; Tolbert, L. M.; Linares-Samaniego, S. *J. Phys. Chem. A* **1997**, *101*, 4602.

(10) *Correlation Analysis in Chemistry*; Chapman, N. B., Shorter, J., Eds.; Plenum Press: New York, 1978.

(11) Kondratenko, N. V.; Popov, V. I.; Kolomeitsev, A. A.; Saenko, E. P.; Prezhdo, V. V.; Lutskii, A. E.; Yagupol'skii, L. M. *USSR J. Org. Chem.* **1980**, *16*, 1049.

(12) Kowalik, J.; VanDerveer, D.; Clower, C.; Tolbert, L. M. *Chem. Commun.* **1999**, *19*, 2007.

(13) Solntsev, K. M. Unpublished work.

(14) A nonlinear least-squares fit to the equation $y = (A_1 - A_2)/(1 + e^{(x-x_0)/dx}) + A_2$ (first-order Boltzmann function) is widely used for the analysis of sigmoid-shaped experimental data, for example, ion-channel $I-V$ relationships: De Weer, P.; Gadsby, D. C.; Rakowski, R. F. *J. Gen. Physiol.* **2001**, *117*, 315.

(15) As compared to the solutions of quinine sulfate in 0.1 N sulfuric acid and anthracene in ethanol as standards with quantum yields of 0.546 and 0.28, respectively. See Demas, J. N.; Crosby, G. A. *J. Phys. Chem.* **1971**, *75*, 991.

(16) **6F3** can be partially dissolved in pure water at pH > 10. Emission spectra have the same shape as the dashed curve in Figure 3, with maxima at 436 nm.

(17) Krissinel, E. B.; Agmon, N. *J. Comput. Chem.* **1996**, *17*, 1085.

(18) A three-exponential fit gives only slightly better results than does a biexponential in helping to bridge ultraslow and ultrafast components.

(19) In the case of biexponential decay when lifetimes differ by two or more orders of magnitude, the measurements should be done at conditions of maximum time resolution to obtain the correct amplitudes of the longer exponents.

(20) (a) Canals, I.; Portal, J. A.; Bosch, E.; Rosés, M. *Anal. Chem.* **2000**, *72*, 1802. (b) Rosés, M.; Rived, F.; Bosch, E. *J. Chromatogr., A* **2000**, *867*, 45. (c) Canals, I.; Oumada, F. Z.; Rosés, M.; Bosch, E. *J. Chromatogr. A* **2001**, *911*, 191.

(21) In recent semiempirical AM1 calculations, Agmon et al. (Agmon, N.; Rettig, W.; Groth, C. *J. Am. Chem. Soc.* **2002**, *124*, 1089.) demonstrated that intramolecular charge migration from the hydroxyl oxygen to the aromatic ring does indeed occur upon excitation of 2-naphthol and its cyano derivatives. The largest excess electronic charge is located, however, on C-5 and C-8 of the distal aromatic ring, which is in agreement with the observation that 5-cyano- and 8-cyano-2-naphthols are stronger photoacids than are other monocyano-2-naphthols.[1,9] Nevertheless, no resonance structure stabilized by 5-substitution can be easily rationalized by a simple valence-bond scheme (Figure 8), and no H/D exchange was ever observed upon irradiation of **N2** in protic deuterated solvents. It is interesting to check whether the enhanced photoacidity of 5-perfluoromethanesulfonyl-2-naphthol, which has been recently synthesized in our group, is accompanied by a decrease of R*OH and $R^*O^-$ fluorescence lifetimes.

(22) Webb, S. P.; Philips, L. A.; Yeh, S. W.; Tolbert, L. M.; Clark, J. H. *J. Phys. Chem.* **1986**, *90*, 5154.

(23) Solntsev, K. M.; Huppert, D.; Agmon, N. *Phys. Rev. Lett.* **2001**, *86*, 3427.

(24) Zaitsev, N. K.; Demyashkevich, A. B.; Kuz'min, M. G. *High Energy Chem.* **1978**, *12*, 361.

(25) Chattopadhyay, N.; Serpa, C.; Pereira, M. M.; de Melo, J. S.; Arnaut, L. G.; Formosinho, S. J. *J. Phys. Chem. A* **2001**, *105*, 10025 and references therein.

(26) Fluorescence lifetimes of **6F3** ($\tau_0 = 1/(k_{nr} + k_f)$) decreased from 4.9 ns in hexane ($E_T = 30.9$ kcal/mol) down to 1.0 ns in acetonitrile ($E_T = 46.0$ kcal/mol) and 0.5 ns in methanol ($E_T = 55.4$ kcal/mol). The fluorescence rate constant $k_f$ has a very weak solvent dependence.

(27) (a) Gopich, I. V.; Solntsev, K. M.; Agmon, N. *J. Chem. Phys.* **1999**, *110*, 2164. (b) Agmon, N. *J. Chem. Phys.* **1999**, *110*, 2175.

(28) Depending on the sign of the expression $\Delta k \equiv k'_0 - (k_0 + k^*_{pt})$, three different behaviors for the "corrected" R*OH signal $F(t) \equiv [R^*OH] \exp(k'_0 t)$ are possible. When the anion is relatively long-lived ($\Delta k < 0$, the usual case for most hydroxyaromatics), $F(t)$ shows fast conversion from the initial exponential into $t^{-3/2}$ decay. In the transition $\Delta k = 0$ regime, $F(t)$ decays slowly and switches into a $t^{-1/2}$ decay. For short-lived anions, $\Delta k > 0$ and $F(t)$ rises exponentially.

(29) (a) Mendicuti, F.; Saiz, E.; Zuniga, I.; Patel, B.; Mattice, W. L. *Polymer* **1992**, *33*, 2031. (b) Kawakami, J.; Komai, Y.; Sumori, T.; Fukushi, A.; Shimozaki, K.; Ito, S. *J. Photochem. Photobiol., A* **2001**, *139*, 71.

(30) Jones, G., II.; Vullev, V. I. *J. Phys. Chem. A* **2001**, *105*, 6402.

(31) Karrer, P.; Leiser, P. *Helv. Chim. Acta* **1944**, *27*, 678.

(32) Fujita, S. *Synthesis* **1981**, 423.

(33) Oae, S.; Togo, H. *Bull. Chem. Soc. Jpn.* **1983**, *56*, 3802.